2014 Health Innovations and Point-of-Care Technologies Conference
Seattle, Washington USA, October 8-10, 2014

Detrended Fluctuation Analysis of Photoplethysmogram Pulse Rate Intervals in Sleep Disordered Breathing*

Parastoo Dehkordi, Ainara Garde, Walter Karlen, Christian L. Petersen, Mark J. Ansermino, and A. Guy Dumont

Abstract— **The fluctuation of heartbeat intervals is irregular and erratic in healthy young individuals. Sleep disordered breathing (SDB) influences the fluctuation of heart rate. In this study, we investigated the effects of SDB on heart rate fluctuations by analyzing the short- and long-range correlation of photoplethysmogram pulse to pulse intervals (PPIs). We recruited 160 children referred to British Columbia Children's Hospital for overnight polysomnography and recorded the photoplethysmogram (PPG) using the Phone Oximeter™. Detrended fluctuation analysis was applied to analyze the scaling behavior of PPIs time series in children with and without SDB. We found stronger short-range (10 to 40 pulses) and long-range (70 to 200 pulses) correlation in children with SDB. This reflects the loss of irregularity of heart rate in children with SDB.**

I. INTRODUCTION

Sleep disordered breathing (SDB) describes a group of disorders characterized by frequent partial or complete cessation of breathing during sleep. Childhood SDB includes children with obstructive sleep apnea syndrome (OSAS) and children with disorders of the respiratory muscles [1]. OSAS, the most prevalent type of SDB, is characterized by periodic interruption of breathing (apnea/hypopnea) during sleep generally caused by a collapse in muscles of the upper airway [2]. The level of severity of SDB is quantified by the observed average number of apneas and hypopneas per hour of sleep (the apnea/hypopnea index (AHI)).

Heartbeat intervals normally fluctuate in irregular and erratic manners [3]. In the healthy children this fluctuation is more erratic than adults. In contrast, ageing and disease are accompanied by the lost of complexity and increased regularity in heart rate fluctuation [3].

The fluctuation of time intervals between consecutive heart beats is induced by nonlinear interaction between the two branches of the autonomic nervous system [4]: the sympathetic and parasympathetic branches. The sympathetic activity increases the firing rate of cardiac pacemaker cells while the parasympathetic activity has the opposite effects [4]. The competition between sympathetic and parasympathetic branches is assumed to be the mechanism which mainly causes the erratic fluctuation of heart rate in healthy subjects. In SDB patients, intermittent sleep fragmentation and disturbance in normal respiration and oxygenation that accompany most apnea/hypopnea events lead to the changes in cardiac autonomic regulation. These changes show itself in the form of reduced parasympathetic activity and prominent sympathetic activity in SDB patients that even continues during wakefulness [5].

In recent years, fluctuation of R-R intervals (RRIs) has received significant attention as a promising non-invasive indicator of cardiac automatic function. Time series of RRIs obtained from electrocardiograms are non-stationary and exhibit short- and long-range fluctuations [6], [7], [8]. The short-range fluctuation is commonly considered to reflect the baroreflex mechanism (0.1 Hz) and also the respiratory sinus arrhythmia (0.15-0.4 Hz), while the long-range fluctuation shows the effort of autonomic nervous system to limit the heart rate [6]. Power spectral analysis of RRIs has been extensively used to characterize short-range fluctuation of heart rate. However, when it is applied to long non-stationary time series it can produce misleading results. To overcome this limitation, Peng et al. introduced the detrended fluctuation analysis (DFA) [8]. DFA detects the short- and long-range correlations in time series expressed as scaling exponents. Peng et al. showed that it was possible to distinguish healthy subjects from those with severe heart failure by looking at the short- and long-term correlations in heartbeat intervals [6]. Later, Penzel et al. investigated the short- and long-range correlation of heart rate intervals measured by DFA in individuals with SDB and found that DFA is better identifying the sleep apnea severity compared to spectral analysis [9].

In our previous studies, we have shown that there was a strong correlation between photoplethysmogram PPIs and electrocardiogram RRIs [10]. Later, we investigated the fluctuation of heart rate through the power spectral analysis of short and stationary segments of PPIs in SDB children and concluded that SDB affected the short-term fluctuation of heart rate [11]. In this study, we have investigated the short- and long-range fluctuation of heart rate through the DFA analysis of PPIs. The PPIs time series were extracted from the PPG signals recorded from children suspected of having SDB using the Phone Oximeter™ [12], [13]. The Phone Oximeter™ is a mobile device that integrates a pulse oximeter with a smartphone. Phones are widely available even in the most remote areas [14] and have become a cornerstone in developing economies and the livelihood of people everywhere. Furthermore, the smartphone portion of the mobile market is set to surpass that of basic and feature

* This work was supported in part by NSERC/ICICS People & Planet Friendly Home Initiative at UBC and NSERC/CIHR under the CHRP program and the Institute for Computing

P. Dehkordi, A. Garde, W. Karlen, C. L. Petersen, J. M. Ansermino and G. A. Dumont are with the Electrical and Computer Engineering in Medicine group (ECEM), and the Pediatric Anesthesia Research Team (PART), The University of British Columbia (UBC), Vancouver, Canada. parastoo.dehkordi at cw.bc.ca

978-1-4799-2918-4/14/$31.00 ©2014 IEEE

phones, driven mainly by the growth in the emerging markets [15]. Thus, the use of the phone as the display and power source of the pulse oximeter can overcome some of the challenges of distributing the technology. Usability studies of the Phone Oximeter™ prototype previously undertaken both in Canada and Uganda gave overall usability scores of 82% and 78% respectively, indicative that a phone can be a functional oximeter interface [16].

II. MATERIALS AND METHODS

A. Subjects

All subjects were recruited according to a protocol approved by the University of British Columbia and Children's and Women's Health Centre of British Columbia Research Ethics Board. One hundred and sixty children referred to the British Columbia Children's Hospital for polysomnography (PSG) recording were enrolled in this study. Children with arrhythmia or abnormal hemoglobin were excluded. The recordings of 14 children were excluded from analysis because the total duration of the sleep time or the collected signals from PSG or the Phone Oximeter^{TM} were shorter than 3 hours. Using the PSG outcomes and diagnostic report of the paediatric respiratory specialist, the subjects were divided into two groups: SDB subjects with AHI more than 5 and non-SDB subjects with AHI less than 5 (Table I).

TABLE I
DEMOGRAPHIC MATRIX AND AHI OF STUDIED DATABASE EXPRESED AS MEAN ± STANDARD DEVIATION

	Total (n = 146)	**non-SDB (n = 90)**	**SDB (n = 56)**
Age (year)	9.1 ± 4.2	9.3 ± 4.0	8.7 ± 4.5
BMI[1](kg/m^2)	20.00 ± 6.4	17.41 ± 6.43	23.00 ± 8.22
AHI	8.40 ± 15.0	1.40 ± 1.20	19.77 ± 19.68

[1] Body Mass Index

B. Data Collection

Standard polysomnography (PSG) recordings were made with the Embla Sandman S4500 (Embla Systems, ON, Canada), specifically designed to meet the American Academy of Sleep Medicine (AASM) accreditation requirements. The recordings included overnight measurements of electrocardiography, electroencephalography, oxygen saturation (SpO_2), photoplethysmogram (PPG), chest and abdominal movement, nasal and oral airflow, left and right electrooculography, electromyography and video recordings. The PSG included post hoc labeling of sleep phases and all events (apnea, hypopnea, arousal, etc.) by a sleep technician (PSG event log file).

In addition to the PSG, the PPG, heart rate, and SpO_2 were recorded simultaneously with the Phone Oximeter™. The pulse oximeter sensor of the Phone Oximeter™ was applied to the finger adjacent to the one used for PSG. The SpO_2 and PPG signals recorded by the Phone Oximeter™ were sampled at 1 Hz and 62.5 Hz, respectively.

C. Pulse Rate Intervals

After baseline removal and smoothing with a Savitzky-Golay FIR filter (order 3, frame size 11 samples), all PPG signals were divided into 5-minute segments with 1-minute overlap. Each segment was classified with a signal quality index [17] and the segments with low signal quality index were automatically rejected from further analysis. In order to obtain the PPIs time series, a simple zero-crossing algorithm was used to locate the pulse peaks in the PPG signals, and the intervals between successive peaks were computed. The PPIs with the length less than 0.33 second and more than 1.5 were concidered unphysiological and deleted from the time series.

All segments were scored as wakefulness, non-REM and REM based on the labels of the 30-s epochs in the PSG event log file. To eliminate the effects of sleep stage transition and non-stationarities associated with them, the segments with any sleep state transition containing multiple sleep state labels (e.g. from wakefulness to non-REM or from non-REM to REM) were removed from the data set.

D. Detrended Fluctuation Analysis

To quantify the short- and long-range of heart rate, we applied DFA to the PPIs time series. DFA detects the internal correlation of signal expressed by scaling properties. To calculate DFA, we followed a four-step procedure [6]:

Step 1: An integrated version of the original pulse-to-pulse interval time series (total pulses = N) was formed:

$$y(k) = \sum_{i=1}^{k} [PPI(i) - PPI_{avg}], \tag{1}$$

where *PPI(i)* was the *i*th PPIs, PPI_{avg} was the mean of PPIs and k = 1,...,N.

Step 2: The time series *y(k)* were divided into equally spaced non-overlapping windows with length *n* (number of pulses in each window).

Step 3: For each window, the local trend $y_n(k)$ was separately calculated by a quadratic least-squares fit.Then the integrated time series *y(k)* was detrended by subtracting the local trend $y_n(k)$.

Step 4: Finally, the root-mean-square fluctuation of the integrated and detrended time series was calculated by

$$F(n) = \sqrt{\frac{1}{N}\sum_{k=1}^{N}[y(k) - y_n(k)]^2}. \tag{2}$$

In order to determine how *F(n)* depends on the time scale *n*, the process was repeated for several time scales *n*. Typically, *F(n)* increases when *n* increases as a power law,

$$F(n) \sim n^{\alpha}. \tag{3}$$

In a double logarithmic plot, the scaling exponent α shows the slope of a line that fits *log(F(n))* to *log(n)*. α = 0.5 corresponds to an uncorrelated time series. $0 < \alpha < 0.5$ is indicative of anti-correlation in time series, which means that

short and large intervals are more likely to alternate. 0.5 $<\alpha$ <1 represents correlation in the time series, which means that short intervals are more likely to be followed by short intervals and vice versa [6].

In short-range correlations, the initial slope differs from 0.5 for small *n*s, but it will approach 0.5 for large *n*s. In persistent long-range correlations α is greater than 0.5 and less than 1 for large *n*.

To determine the short- and long-range correlation in PPIs sequences, we defined α_S and $\alpha_L$as the slope of *log(F(n))* as a function of *log(n)* for the range 10 $\leq$ n $\leq$ 40 to represent the short-range correlation, and for the range 70 $\leq$ n $\leq$ 200 to represent the long-range correlation, respectively [9]. We compared α_S and α_L in children with and without SDB using the Wilcoxon rank rum test.

III. RESULTS

In a double logarithmic representation, α, the slope of *F(n)* in the range of 10 $\leq$ n $\leq$ 200, was larger for the SDB children compared with the children without SDB (Figure 1). Both α_S and α_L for children with SDB were larger than for children without SDB (Figure 2). However, α_L changed much more significantly than α_S (Table II). The histogram of α_L for children with SDB is centered on 0.60 $\pm$ 0.12 and for children without SDB is centered on 0.67 $\pm$ 0.13. For all children, α_S was observed to be larger than α_L (Table II).

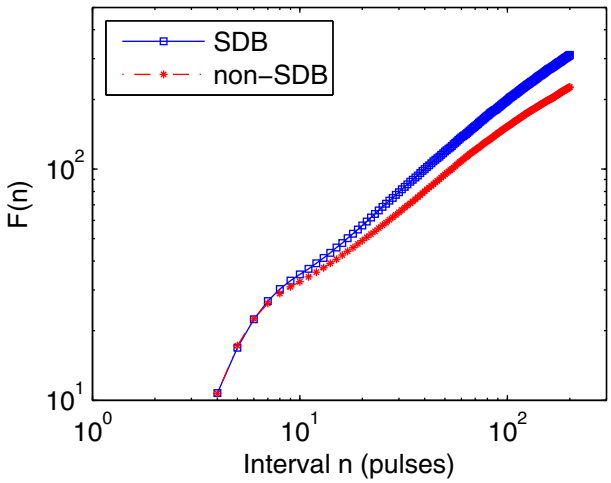

Fig. 1. The double logarithmic presentation of fluctuation function F(n) versus window size n (4 to 200 pulses) in entire sleep for children with and without SDB

IV. DISCUSSION

In this study we investigated the short- and long-range correlation of heart rate through DFA analysis of photoplethysmogram PPIs in children with and without SDB. Our findings suggest that the short- and long-range fluctuation of heart rate is more strongly correlated in SDB children compared with non-SDB children.

α_S and α_L were used to quantify the short- and long-range correlation of PPIs time series respectively. We found

TABLE II

THE COMPARISON BETWEEN DIFFERENT TIME SCALING EXPONENTS IN CHILDREN WITH AND WITHOUT SDB (SDB AND NON-SDB RESPECTIVELY

	non-SDB (Median)	**SDB (Median)**	**mean difference**	**95% CI (Low, High)**	**P-value**
α	0.68	0.74	0.062	0.009, 0.112	0.01
α_S	0.7	0.82	0.089	0.014, 0.163	0.01
α_L	0.6	0.68	0.081	0.034, 0.125	0.0003

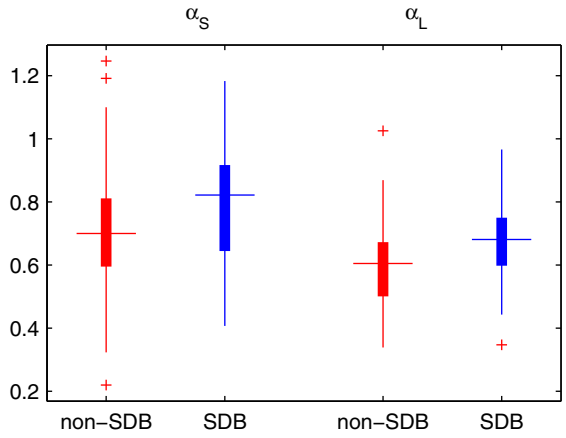

Fig. 2. The boxplots show α_S and α_L for children with and without SDB. α_S is the slope of log(F(n)) as a function of log(n) in the range 10 $\leq$ n $\leq$ 40 and α_L is the slope of log(F(n)) as a function of log(n) in the range 70 $\leq$ n $\leq$ 200. Lower quartile, median, and upper quartile values were displayed as bottom, middle and top horizontal line of the boxes. Whiskers were used to represent the most extreme values within 1.5 times the interquartile range from the quartile. Outliers (data with values beyond the ends of the whiskers) were displayed as crosses.

that in the SDB group, both α_S and α_L were larger relative to the group without SDB. Since the short-range correlation is associated with the effects of breathing on heart rate, we would argue that the larger α_S value is evidence that the control of heart rate in the range of respiratory related time scales (10 $\leq$ n $\leq$ 40) is much tighter in SDB children. Furthermore, as mentioned by Khoo et al. [5], in patients with SDB the respiratory modulation is not limited to high frequency band (0.15 - 0.4 Hz) associated with respiratory sinus arrhythmia. In SDB, respiration modulation of heart rate takes the form of large cyclical variation that correlates with episodic apnea or hypopnea and mostly elevates the components of very low frequency band ($<$ 0.04 Hz, VLF). The larger α_L we found for SDB children in this study is consistent with elevated VLF band.

In the study by Penzel et al. [9], the short- and long-range correlations of heart rate intervals measured by DFA investigated in adults during different sleep stages. They found α_S = 1.00 and α_L = 0.67 for adult subjects without SDB (age = 33.0 $\pm$ 6.4) during whole sleep. These values are larger than our finding for children without SDB (age = 9.1 $\pm$ 4.2). This suggests that the fluctuation in the RRIs of non-SDB adults is more strongly correlated than the fluctuation in PPIs of non-SDB children. These findings are consistent

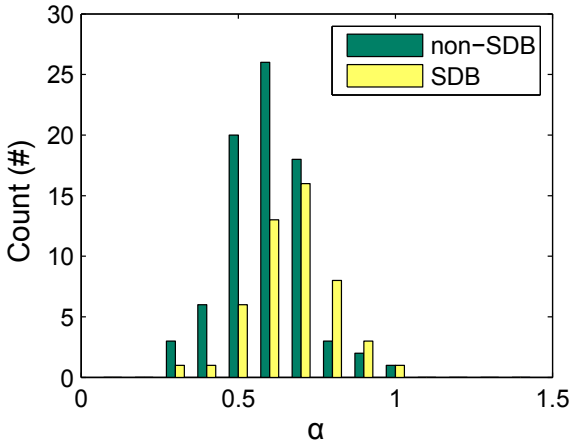

Fig. 3. The histogram of α_L for children with and without SDB. The histogram of α_L for children with SDB is centered on 0.60 ± 0.12 and for children without SDB is centered on 0.67 ± 0.13.

with existing litreture [3], [6].

The findings of this study along with our previous results based on spectral analysis of PPIs [10], [11] confirm that SDB affects the normal fluctuation of PPIs of PPG in a linear as well as nonlinear manner. Furthermore, we have previously shown that the characterization of overnight SpO_2 pattern measured by the Phone Oximeter™ successfully identifies children with significant SDB [18]. Hence, combining SpO_2 and PPIs analysis (both recorded by the Phone Oximeter™) holds promise as a low-cost approach to automatically assess SDB at home. This can greatly increase the accessibility to sleep apnea screening and improve the quality of life for the many millions around the world currently affected by SDB related disorders.

ACKNOWLEDGMENT

The authors acknowledge the contributions of the Medical Day Unit at BC Childrens Hospital and research assistants of the Pediatric Anesthesia Research Team for their assistance in conducting the study.

REFERENCES

[1] C. L. Marcus, "Sleep-disordered breathing in children," *American Journal of Respiratory and Critical Care Medicine*, vol. 164, pp. 16–30, 2001.

[2] A. Malhotra and D. P. White, "Obstructive sleep apnoea," *Lancet*, vol. 360(9328), pp. 237–45, 2002.

[3] A. L. Goldberger, D. R. Rigney, and W. B. J, "Science in pictures: Chaos and fractals in human physiology," *Scientific American*, vol. 262, pp. 43–9, 1990.

[4] G. J. Tortora and S. R. Grabowski, *Principle of Anatomy and Physiology*. John Wiley & Sons, Inc., 2003.

[5] A. Khoo, Michael C. K.; Blasi, "Sleep-related changes in autonomic control in obstructive sleep apnea:a model-based perspective," *Respiratory Physiology & Neurobiology*, vol. 188(3), pp. 267–76, 2013.

[6] C. Peng, S. Havlin, J. Hausdorff, J. Mietus, H. Stanley, and G. AL., "Fractal mechanisms and heart rate dynamics. long-range correlations and their breakdown with disease," *The Journal of Electrocardiology*, vol. 28, pp. 59–65, 1995.

[7] P. C. Ivanov, "Long-range dependence in heartbeat dynamics," *Lecture Notes in Physics (Springer:Berlin)*, vol. 621, pp. 339–68, 2003.

[8] C. K. Peng, J. Mietus, J. M. Hausdorf, S. Havlin, H. E. Stanley, and A. L. Goldberger, "Long-range anticorrelations and non-gaussian behavior of the heartbeat," *Physical Review Letters*, vol. 70, pp. 1343–6, 1993.

[9] T. Penzel, J. Kantelhardt, L. Grote, J. Peter, and A. Bunde, "Comparison of detrended fluctuation analysis and spectral analysis for heart rate variability in sleep and sleep apnea," *IEEE Transactions on Biomedical Engineering*, vol. 5(10), pp. 1143–51, 2003.

[10] P. Dehkordi, A. Garde, W. Karlen, D. Wensley, J. M. Ansermino, and G. A. Dumont, "Pulse rate variability compared with heart rate variability in children with and without sleep disordered breathing," in *Conf. Proc. IEEE Engineering in Medicine and Biology Society*, 2013, pp. 6563–6.

[11] ——, "Pulse rate variability in children with sleep disordered breathing in different sleep stages," in *Conf. Proc. Computing in Cardiology*, 2013, pp. 1015–18.

[12] W. Karlen, G. Dumont, C. Petersen, J. Gow, J. Lim, J. Sleiman, and M. Ansermino, "Human-centered phone oximeter interface design for the operating room," in *Conf. Proc. Health Informatics*, 2011, pp. 433–8.

[13] C. Petersen, T. Chen, J. Ansermino, and D. GA., "Design and evaluation of a low-cost smartphone pulse oximeter," *Sensors*, vol. 13(12), pp. 16 882–93, Dec 2013.

[14] The United Nations Foundation, and Vodafone Partnership, "mhealth for development: The opportunity of mobile technology for healthcare in the developing world," 2009.

[15] NDP DisplaySearch, "Smartphone quarterly," Santa Clara, CA, USA, 20 May 2013.

[16] J. Hudson, S. Nguku, J. Sleiman, W. Karlen, G. Dumont, C. Petersen, C. Warriner, and J. Ansermino, "Usability testing of a prototype phone oximeter with healthcare providers in high- and low-medical resource environments," *Anesthesia*, vol. 67, pp. 957–67, 2012.

[17] W. Karlen, K. Kobayashi, J. M. Ansermino, and G. A. Dumont, "Photoplethysmogram signal quality estimation using repeated gaussian filters and cross-correlation," *Physiological Measurement*, vol. 33, pp. 1617–29, 2012.

[18] A. Garde, W. Karlen, P. Dehkordi, D. Wensley, J. M. Ansermino, and G. A. Dumont, "Oxygen saturation in children with and without obstructive sleep apnea using the phone-oximeter," in *Conf. Proc. IEEE Engineering in Medicine and Biology Society*, 2013, pp. 2531–4.